TiO$_2$-ZrO$_2$ Binary Oxides for Effective Hydrodesulfurization Catalysts

R. Tiwari, B.S. Rana, R. Kumar and A.K. Sinha[*]

Indian Institute of Petroleum, Mohkampur, Dehradun 248005, India

Abstract: Titania-zirconia mixed oxide was developed as support for Mo, CoMo and NiMo catalysts. Synthesis was carried out using evaporation induced self assembly and modified sol-gel templating route. The samples were calcined in a temperature range of 400°C to 600°C. SEM and porosity analyses were used to ensure that the mesostructure is stable after Mo and promoter incorporation. Wide-angle XRD was used to verify MoO$_3$ (and MoS$_2$) dispersion, which indicated crystallite size <40Å up to 8wt% Mo loading. The IR spectral studies were used to determine the nature of Mo species (octahedral and tetrahedral). TPD study was used to determine the acidity of the supports. The physico-chemical properties were correlated with the catalytic hydrodesulfurization reaction. CoMo and NiMo catalysts were compared in order to gain an insight into the promoter effect on direct desulfurization pathways. A comparison with γ-Al$_2$O$_3$, SBA-15 and KIT-6 supported catalysts shows much superior activities of mesoporous titania-zirconia supported catalysts which is attributed to favorable metal-support interactions in case of mesoporous titania-zirconia supported catalysts.

Keywords: Hydrodesulfurisation, titania-zirconia mixed oxides, promoter effect.

1. INTRODUCTION

Increasing awareness of the impact on environmental pollution by automobiles has shifted the responsibility of pollution control to the refineries side. As a consequence of this, the gasoline and diesel sulfur specifications are made increasingly stringent. The sulfur level is expected to be lowered all over the world, to less than 10 ppm for gasoline and diesel and 0 ppm for fuel cell application range. To achieve such low sulfur levels in fuels, the activity of the present catalyst need to be increased by about 7 to 10 times. In order to reach such low level sulfur many approaches are required among which variation of support is an important one. In modern refinery, sulphur in fuels is removed by means of hydrotreating process, in which the hydrodesulfurisation catalyst is the core of the technique. Due to increasingly heavier crudes, it has however become difficult to achieve the future sulfur specification with current catalysts and processes [1]. To meet the challenges related to the HDS of various petroleum fractions, development of newer generation of catalysts is necessary. There have been various attempts to improve catalyst activity such as changes in active metal composition, use of different types of active metals, additives and supports etc. among which variation of support is an important one [2-4]. Most of the HDS catalysts employed for industrial applications are molybdenum based promoted with cobalt and nickel and supported on alumina. Other materials have also been tried as supports for hydrotreating catalysts such as various oxides [5, 6] like SiO$_2$, MgO, ZrO$_2$, TiO$_2$, and mixed oxides derived from above-mentioned oxides [7-10], carbon [11], clays [12], mesoporous materials like MCM-41[13-15], HMS [16], SBA-15 [17], zeolites like Na–Y, USY [18, 19]. Kumaran *et al*. [20, 21] reported Al-SBA-15 of various Si/Al

ratio for HDS of thiophene and suggested that Al containing SBA-15 supported catalysts displayed higher activities than the γ-Al$_2$O$_3$ supported catalysts. Similar results have been reported by Chiranjeevi *et al*. [22] for Al-HMS supported Mo catalysts. Vradman *et al*. [23] reported higher activities for HDS and hydrogenation (HYD) using NiW/SBA-15 catalysts.

Reddy *et al*. [24] showed that MCM-41 can be an effective support for hydrodesulfurization catalysts. Corma *et al*. [25] have reported that mesoporous aluminosilicate MCM-41 is a good catalyst for mild hydrocracking of gas oil. A combination of large surface area, large pore size to allow diffusion of bulky molecules, together with the presence of mild acidity and high stability, result in superior HDS, HDN and hydrocracking performance than zeolite and alumina supported catalysts.

Sampieri *et al*. [26] prepared MoS$_2$/SBA-15 and MoS$_2$/MCM-41 catalysts with various Mo loading by mechanical mixing followed by thermal spreading without serious damage to the support structure. His findings showed that in case of SBA-15 supported catalyst the MoS$_2$ slabs were randomly oriented in the pores of the support and an average MoS$_2$ slab length of 2.8 nm and a stacking of 2 was determined. However in case of MCM-41 supported catalysts, MoS$_2$ slabs blocked the relatively smaller mesopores resulting in comparatively lower activity than for SBA-15 supported counterparts. Different mixed oxides have been employed as supports for hydrotreating catalysts. SiO$_2$, MgO, TiO$_2$, ZrO$_2$ and their mixed oxides with Al$_2$O$_3$ have been reported to possess interesting range of textural properties as well as different kind of active metal interactions with the support. The effect of support on catalyst activity has already been subject of several papers. However, these catalysts could not be commercially exploited due to their low surface area, limited thermal stability and unsuitable mechanical properties. To get more insight into the role played by the Ti, in Ti containing

*Address correspondence to this author at the Indian Institute of Petroleum, Mohkampur, Dehradun 248005, India; Tel: 91-135-2525842; Fax: 91-135-266901; E-mail: asinha@iip.res.in

supports, a number of authors followed several methods like grafting of TiO_2 on Al_2O_3, SiO_2, etc. and forming mixed oxides of TiO_2 with other oxides such as Al_2O_3, SiO_2, ZrO_2. Among these mixed oxides TiO_2–Al_2O_3 systems received maximum attention while TiO_2–ZrO_2 and TiO_2–SiO_2 are comparatively less studied. In the case of TiO_2–ZrO_2 and TiO_2–Al_2O_3 the activities obtained are considerably higher than constituent single oxides, indicating that some kind of synergistic action of the two constituents of the support which has led to an activity increase. Similar kind of synergy is observed for SiO_2–TiO_2 supported catalysts [27].

In the present work with the aim of increasing the HDS activity of molybdenum catalysts, we prepared TiO_2-ZrO_2 oxides by employing a modified sol-gel and evaporation induced self assembly technique and investigated the effect of calcination temperatures on the textural properties of the oxides. A series of titania-zirconia supported Mo, CoMo, NiMo catalysts were developed with Mo in varying compositions (8wt%, 10wt% and 12wt%) and Ni and Co loading were varied from 2wt% to 4wt%. The catalysts were evaluated for hydrodesulfurization of thiophene. CoMo and NiMo catalysts were compared in order to gain an insight into the promoter effect on direct desulfurization pathways. Thiophene HDS was chosen as the model reaction for testing the catalytic activities. Characterization of TiO_2-ZrO_2 binary metal oxides was done using techniques like BET surface area, XRD, SEM, FTIR, TGA-DTA etc. Generally single oxide supported catalysts are known to have lower activity for hydrotreating compared to mixed oxide supports. Several reasons like increased acidity, increased dispersion of active phase, improved sulfidability or reducibility, state of promoters etc. have been suggested for the good performance of Ti containing mixed oxide HDS catalysts [28-33]. Activities of the above catalyst were compared with γ-Al_2O_3, SBA-15 and Al-SBA-15 supported Mo, CoMo, and NiMo catalyst.

2. EXPERIMENTAL

2.1. Synthesis

Modified sol-gel technique and evaporation induced self assembly route was employed for synthesis of TiO_2-ZrO_2 binary oxides. In a typical process 7.5gm of P-123 block co-polymer (Sigma-Aldrich) was added to 100ml of absolute alcohol with continuous stirring until a transparent homogenous solution was obtained. To this solution 1.637gm of Zirconium isopropoxide (Acros) was added drop-wise with vigorous stirring. When whole of Zirconium isopropoxide was well dispersed, 28.84 gm of Titanium isopropoxide (Acros) was added to the above solution and the whole content was stirred for an hour at room temperature. Typical gel composition was - 60Ti: 4Zr : 2, 3 P-123: 1110 Ethanol. The solution was then transferred onto an open petridish and left for ageing at 40°C for 7 days. So obtained sample was extracted in acidic ethanol, filtered and dried at 110°C and finally calcined at 500°C for 2 hours (1°C/min). Several titania-zirconia (TZ) supports were prepared – low template samples: TZ-2(400), TZ-2(500), TZ-2(600); high template samples: TZ-3(400), TZ-3(400), TZ-3(500), TZ-3(500).

The NiMo and CoMo catalysts were prepared by incipient wetness impregnation method using an appropriate amount of ammonium heptamolybdate dissolved in ammonia solution. The Ni-promoted and Co-promoted catalysts were also prepared by similar procedure using the dried Mo supported catalysts. Nickel nitrate salt and Cobalt nitrate salts dissolved in water at a constant pH of 6 were used to load Ni and Co on Mo-supported catalysts. The final catalysts were dried at 110°C overnight and calcined at 500°C for 2 hours.

2.1.1. Characterization

The catalysts and supports were characterized by X-ray diffraction (XRD), scanning electron microscopy (SEM), TGA-DTA, NH_3-TPD, and IR studies. X- ray diffraction pattern were obtained using CuKα radiation (40kV and 40mA). Scanning electron microscope (SEM) images were obtained on FEI, Quanta 200F (Netherlands). The porous properties of metal loaded catalysts were studied by N_2 adsorption–desorption isotherms at 77 K (Belsorb Max, BEL, Japan) and the related data (surface area, S_{BET}; pore volume, V_P; pore diameter, Dp) were calculated. IR analyses were carried out by mixing the powdered sample with KBr and making it into a thin wafer of 13 mm diameter. Each sample was scanned for 20 times at a resolution of 2 cm^{-1}, and the average spectrum was taken. The amount and strength of the acid sites were measured by ammonia adsorption-desorption technique using a chemical adsorption instrument, Micrometrics 2900 with a thermal conductivity detector. About 0.10 g sample was saturated with NH_3 at 120 °C, then flushed with helium to remove the physically adsorbed NH_3, finally the desorption of NH_3 was carried out at a heating rate of 10 °C/min in helium flow.

2.2. Activity Determination

We prepared a series of binary oxides and studied the HDS activity using meso-TZ-2500 as the catalyst support. Thiophene hydrodesulfurization (HDS) was chosen as the model reaction for testing the catalytic activities. A glass differential-flow micro-reactor, operating under normal atmospheric pressure and interfaced to a gas chromatograph by a six-way gas-sampling valve, was used to measure the activities of the catalysts. In a typical experiment about 0.1 g of a catalyst sample secured between two plugs of quartz wool inside the glass reactor (Pyrex glass tube, 0.8 cm i.d.) was sulfided at 400°C for 2 h. Sulfidation was carried out using a mixture of CS_2 and H_2 (10% CS2 and 90% H2) at a flow rate of 40 ml/min. After the sulfidation at 400°C for 2 h the temperature was maintained at the reaction temperature and CS_2/H_2 gas flow was stopped. The catalyst was flushed at this temperature with H_2 until no CS_2 could be detected in the effluent gas. Thiophene feed was introduced through the gas bubblers. Thiophene (99.9%) or cyclohexene (99.9%) feeds at 25°C were introduced through gas bubblers. Initial concentrations of thiophene and cyclohexene were 16.3% and 7.7% respectively. The catalyst was taken in powder form to minimize internal and external diffusion effects. The rate can be calculated directly from the equation-

X = r (F/ W),

where r is the rate in mol $h^{-1}g^{-1}$ catalyst, X is the fractional conversion, W is the weight of catalyst in gram and F is the total flow rate of reactant gas in mole h^{-1}. The conversions were kept below 15% to minimize diffusional problems.

The reaction products of thiophene were analyzed by gas chromatograph. For thiophene the column temperature was maintained at 80°C. The reaction products of thiophene are butane, 1-butene, 2-butene and its isomer, and trace amount of 1,3-butadiene. A carrier gas (nitrogen) flow of 40 cc min^{-1} was maintained and a flame ionization detector (FID) was used for detection of the reaction products.

3. RESULTS AND DISCUSSION

3.1. Characterization of Support and Supported Catalysts

3.1.1. X-Ray Diffraction Analysis

The wide angle XRD patterns are shown in Fig. (**1a**, **b**). The diffractograms of the catalysts are dominated by anatase phase of titania and there were no peaks due to ZrO₂. This phenomena explains the homogenous dispersion of zirconia in titania matrix. No characteristic peaks of any impurities are detected as also revealed in EDX (Fig. **2**). Characteristic peak of anatase appears at 2Θ= 25.25°, 37.7°, 47.9°, 62.6° 75.1°. Up to 8wt% MoO₃ loading, no new peaks due to bulk MoO₃ are observed. Samples containing 10 wt% and higher MoO₃, show peak at 2Θ= 27.2° due to MoO₃. The results of XRD analyses indicate that up to 8 wt% Mo-loading, MoO₃ remains on the TiO₂-ZrO₂ support as amorphous phase indicating that MoO₃ is well dispersed on the support. The effect of temperature of calcination on the morphology of the titania-zirconia support was also examined in the temperature range of 400°C-600°C. Calcination of the samples was performed for two hours at three different temperatures: 400°C, 500°C, 600°C. Fig. (**1b**) shows the wide angle diffractograms of the supports calcined at three different temperatures. Meso TZ-2(500) exhibits diffraction peaks attributed to anatase titania. With increase in calcination temperature to 600°C, the diffraction pattern becomes narrow and intense indicating a further growth in the size of anatase nanocrystals, which results in collapse of the meso structure. This is also in agreement with the observations reported by Yuan *et al.* [33]. More intense diffraction patterns are observed for the TiO₂-ZrO₂ sample prepared with higher template content indicated as TZ-3 (Fig. **1b**, **d-f**) than that for the TZ-2 series of samples prepared with lower template content The results indicate that besides template content, optimum calcinations temperature has a major role to play in controlling the crystallinity of the porous metal oxides. It has been well established that the number, strength and nature of surface acid sites of catalysts are affected by the catalyst structure which is altered with calcinations temperature [34].

3.1.2. N₂ Sorption Analysis

The porous properties of TiO₂-ZrO₂ and metal loaded catalysts were examined by N₂ adsorption-desorption isotherms at 77K. The N₂ adsorption-desorption isotherms are shown in Fig. (**3**) and the related data (surface area S$_{BET}$, pore volume V$_P$ and pore diameter D$_P$) are presented in Table **1**. Fig. (**4a**, **b**) shows the pore size distribution of the catalysts. The isotherm in Fig. (**3**) exhibits typical type IV pattern with hysteris loop, a typical characteristic of mesoporous materials according to the IUPAC standards. However, the exact shape of loop varies from one catalyst to another which indicates that the geometry of pores is not the
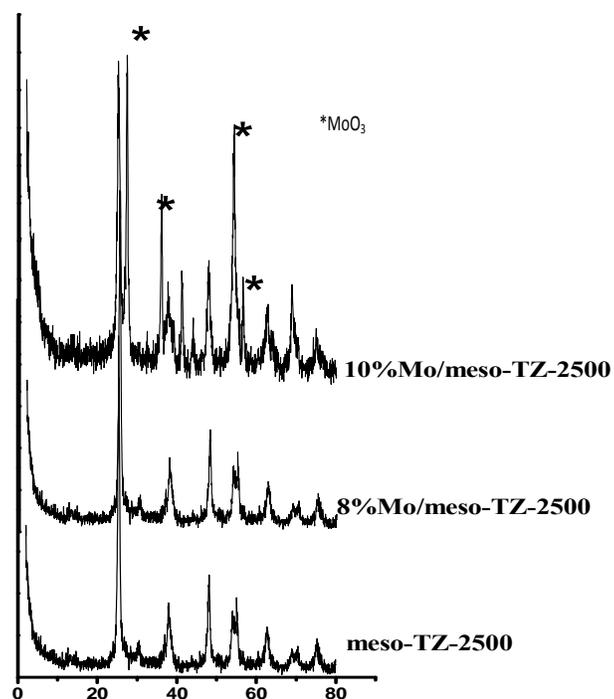
Fig. (1a). Wide angle XRD of the bare and loaded meso-TZ-2(500) catalysts calcined at 500°C.
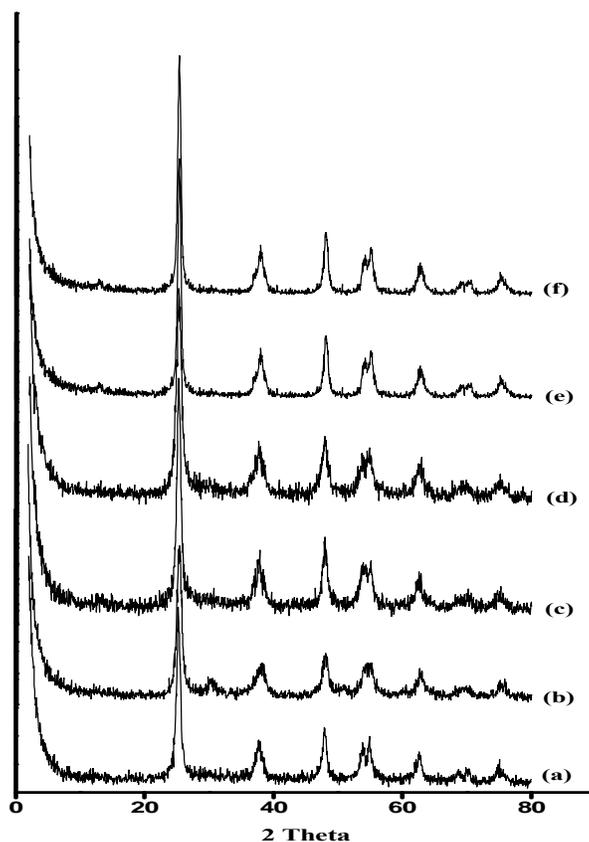
Fig. (1b). Wide angle XRD of (a) TZ-2(400) calcined at 400°C (b) TZ-2(500) calcined at 500°C (c) TZ-2(600) calcined at 600°C (d) TZ-3(400) calcined at 400°C (e) TZ-3(500) calcined at 500°C (f) TZ-3(600) calcined at 600°C.

same for all the catalysts. The pore sizes of meso-TZ-2(500) support and NiMo and CoMo catalysts were calculated using Barrett-Joyner-Halenda (BJH) method. The surface areas of meso-TZ-2(500), CoMo-TZ-2(500) and NiMo-TZ-2(500) are found to be 63.8 m²/g, 49.9 m²/g and 55.2 m²/g respectively. Decrease in surface area with metal loading may be due to the pore blockage of the support. Pore volume results also agreed with this observation. It appears that as Mo is added to the support, well dispersed molybdenum oxide patches are formed as a result of interaction with the hydroxyl group of the support. A sharp increase in adsorption volume of N_2 was observed between 0.5-0.7nm of relative partial pressure which may be attributed to the capillary condensation, showing that pores of the samples are quite homogenous. The effect of calcination temperature on the specific surface areas of the samples were also observed. After calcinations at higher temperature, the specific surface areas decrease quickly. The BET surface areas of 55.0 m²/g, 63.8 m²/g and 3.2m²/g are obtained for the low template content samples calcined at 400°C, 500°C and 600°C respectively. Similar kind of behavior is obtained for high template content samples also where the surface areas drastically reduce to 2 m²/g from 78.3m²/g for calcinations carried out at 600°C and 400°C respectively. These results indicate the breakdown of meso-structures at higher temperature treatment.
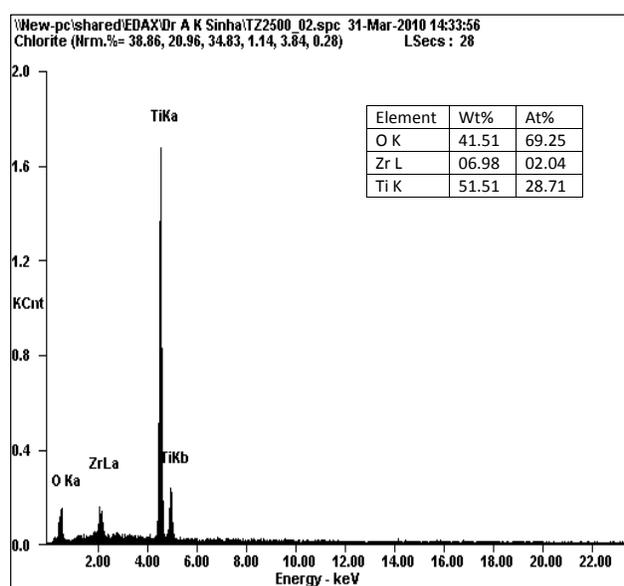
Fig. (2). EDX composition of unloaded meso-TZ-2(500).

3.1.3. FTIR Analysis

Infrared spectra are useful to ascertain the presence of various molybdates. The IR spectra of meso-TZ- 2(500), bare and loaded with molybdenum oxide is shown in Fig. (**5**). The framework region of the IR of the mesoporous samples consist of bands across 3440 cm⁻¹- 3451 cm⁻¹ and may be attributed to the presence of bonded hydroxyl groups. Introduction of Mo into the structure creates new features around 2360 cm⁻¹, 2339.1 cm⁻¹, 862.6 cm⁻¹ and 991.6 cm⁻¹. The features in this region are generally due to the presence of tetrahedral molybdenum, octahedral molybdenum and
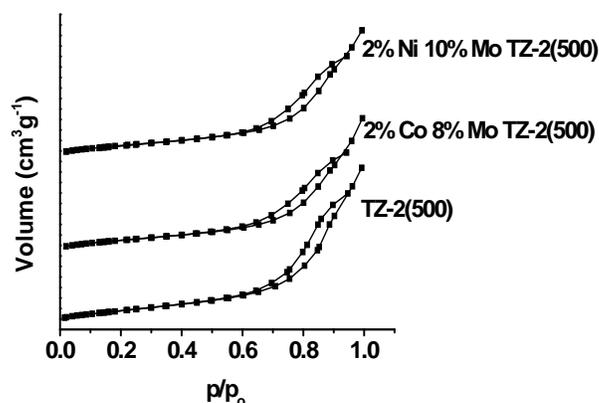
Fig. (3a). Adsorption-desorption isotherms and BJH plots of (**a**) meso-TZ-2(500) (**b**) 2% Co 8% Mo/TZ-(2500) (**c**) 2% Ni 10% Mo/TZ-2(500).
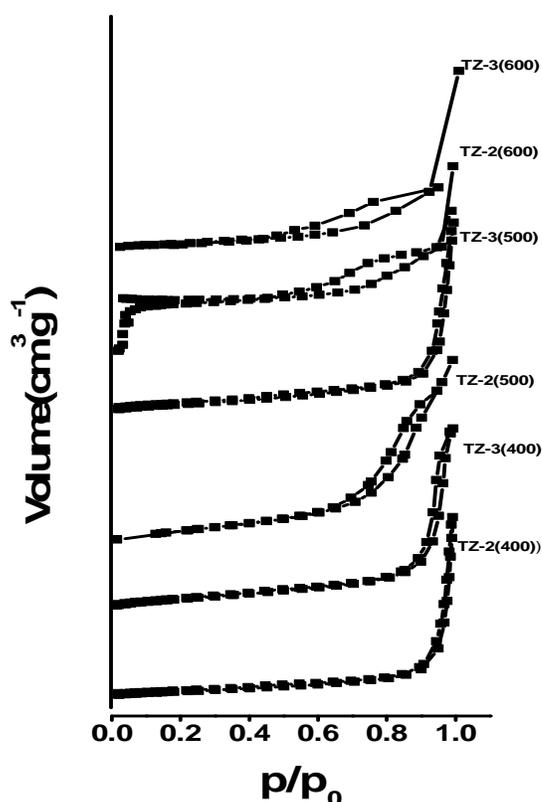
Fig. (3b). Adsorption – desorption plots of catalysts calcined at different temperatures.

Table 1.   Porous Properties of Titania-Zirconia Samples

Sample Composition	S_{BET} (m²/g)	Pore Volume (cm³g⁻¹)	Average Pore Diameter (nm)
TiO₂-ZrO₂ oxide (TZ-2500)	62.00	0.2358	15.21
2%Co8%Mo onTZ-2500	47.97	0.1770	14.75
2%Co10%Mo onTZ-2500	53.40	0.1900	14.23
2%Ni10%Mo onTZ-2500	55.69	0.1969	14.14
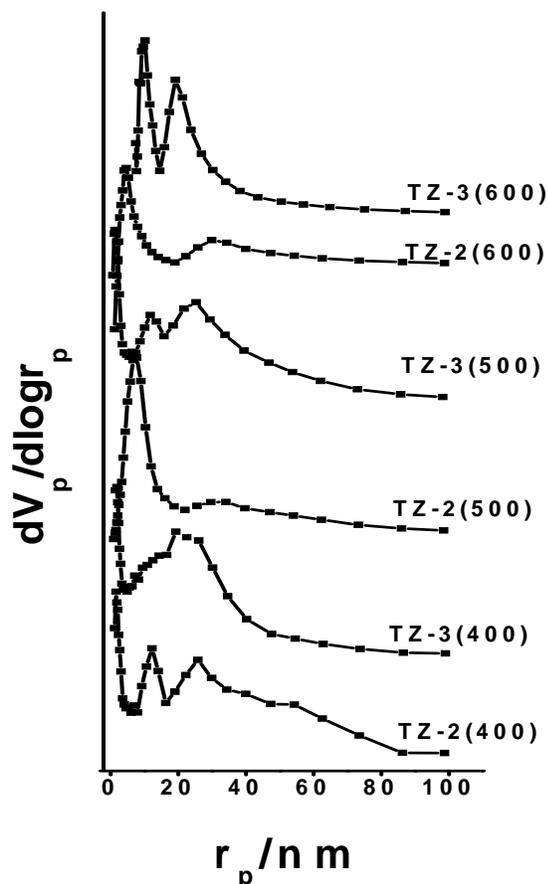
Fig. (4a). Pore size distribution of binary titania –zirconia oxides calcined at different temperatures.
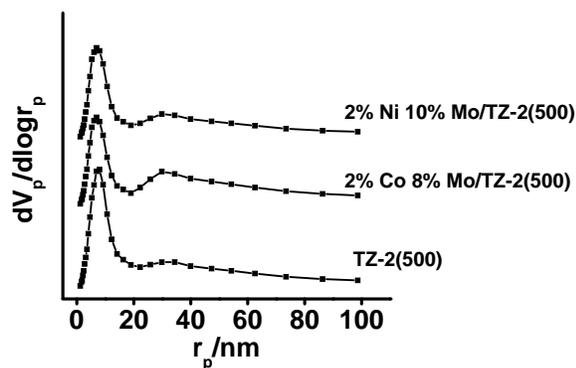
Fig. (4b). Pore size distribution of bare and loaded meso-TZ-2(500) catalysts calcined at 500°C.

other polymolybdates and crystalline MoO_3. Generally the IR spectrum of bulk MoO_3 shows absorption band at 1000cm^{-1} due to M=O stretching vibration mode. With the addition of Mo oxide onto the binary metal oxide support prominent peaks appear around 862.1cm^{-1} and 990-992 cm^{-1}, which are attributed to the presence of octahedral polymeric molybdates [35]. Small bands around 450-590 cm^{-1} may be assigned to the presence of zirconia phases. Bands at 1629-1630 cm^{-1} may be attributed to the undissociated water molecules co-ordinated to surface cationic centres suggesting interactions between

adsorbed water and surface cationic species in the mixed oxides which is in agreement with the observation of Barrera *et al.* [36].
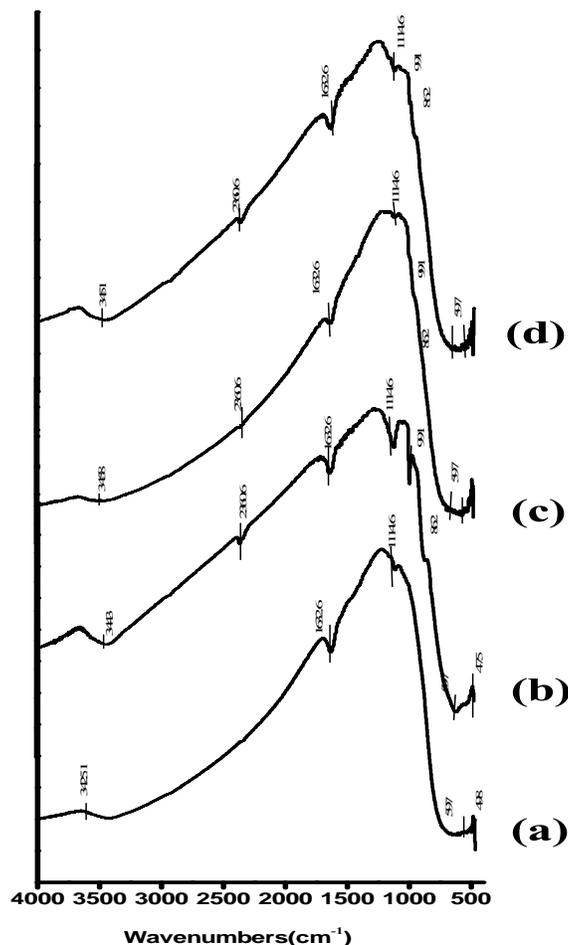
Fig. (5). FTIR of (**a**) TZ-2(500) support (**b**) 8% Mo/TZ-2(500) (**c**) 10% Mo/TZ-2(500) (**d**) 12% Mo/TZ-2(500).

3.1.4. SEM

In order to understand the morphological features the samples were analyzed using SEM. Fig. (**6**) shows the scanning electron micrographs of the calcined samples. As represented in the Fig. (**6a**) under high resolution meso-TZ-2(500) is made of large particles formed due to aggregation of nanograins. The surface shows good uniformity and microparticles appear to be of similar size (~500 nm) when examined at lower resolution (Fig. **6b**). Fig. (**6c**) shows the SEM image of NiMo catalyst with 10% Mo loading and 2% Ni as promoter. Fig. (**6d**) shows the SEM image of catalyst with 8% Mo and 2% Co loading. The two images are more or less similar to the image 6b for the pure support.

3.1.5. TGA-DTA

Fig. (**7**) shows the TG-DTA analysis of bare and metal loaded TZ-2(500). The calcined samples undergo negligible weight loss as expected, thus confirming that the calcination process has completely removed the surfactants that were employed during the synthesis. Slight weight loss at 40-30°C
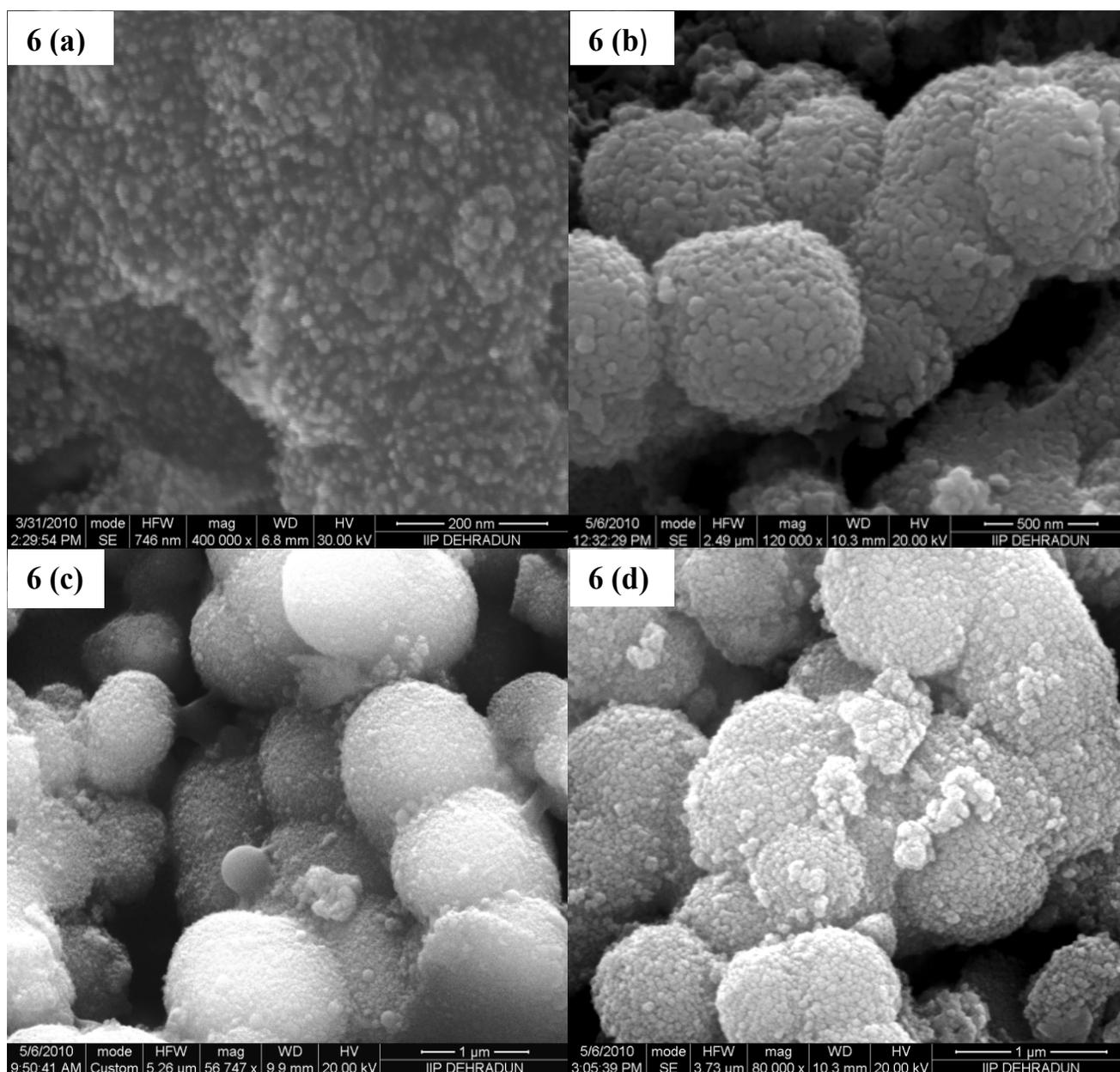
Fig. (6). SEM images of (**a**) meso-TZ-2500 low resolution (**b**) meso-TZ-2500 magnified (**c**) 2% Ni 10%Mo/TZ-2500 (**d**) 2% Co 8% Mo/TZ-2500.

can be attributed to the presence of physisorbed water and at 225-280°C may be due to removal of surface hydroxyl groups. The DTA analysis shows that the samples are stable up to temperature as high as 800°C and phase change (anatase to rutile titania) is not markedly visible. This is also in line with the XRD patterns wherein no peaks due to rutile titania have been identified. However a very broad hump at 745-775°C can be assigned to the transformation of phases, though not very distinct in our case [37]. The phase change delay to 800°C could be related to the stabilization of titania matrix by zirconia and phase segregation between the two oxides might lead to delayed transformation [38]. No exothermic peaks due to ZrO_2 (indicating the presence of monoclinic and tetragonal phases) were observed indicating that the content of ZrO_2 is so less that it gets well embedded into the titania matrix and is so modified that it differs in behavior from that of the pure zirconia.

3.1.6. TPD Analysis

Fig. (**8a**) shows the desorption profile of the catalysts calcined at 400°C, 500°C and 600°C. Concerning the strength of acid sites, usually it is accepted that the desorption temperature can be related to the strength of the sites. It is observed that for all the three temperatures, the maximum desorption is found to occur between 100°C-400°C. Very less desorption occurs at higher temperatures indicating that the samples are moderately acidic. Fig. (**8b**) shows the TPD profile of the catalysts which were employed for hydrotreating. The total acidity of meso-TZ-2(500) is 0.0289 mmolg^{-1} which slightly changes to 0.0275 mmolg^{-1} on Mo impregnation and is almost same for CoMo and
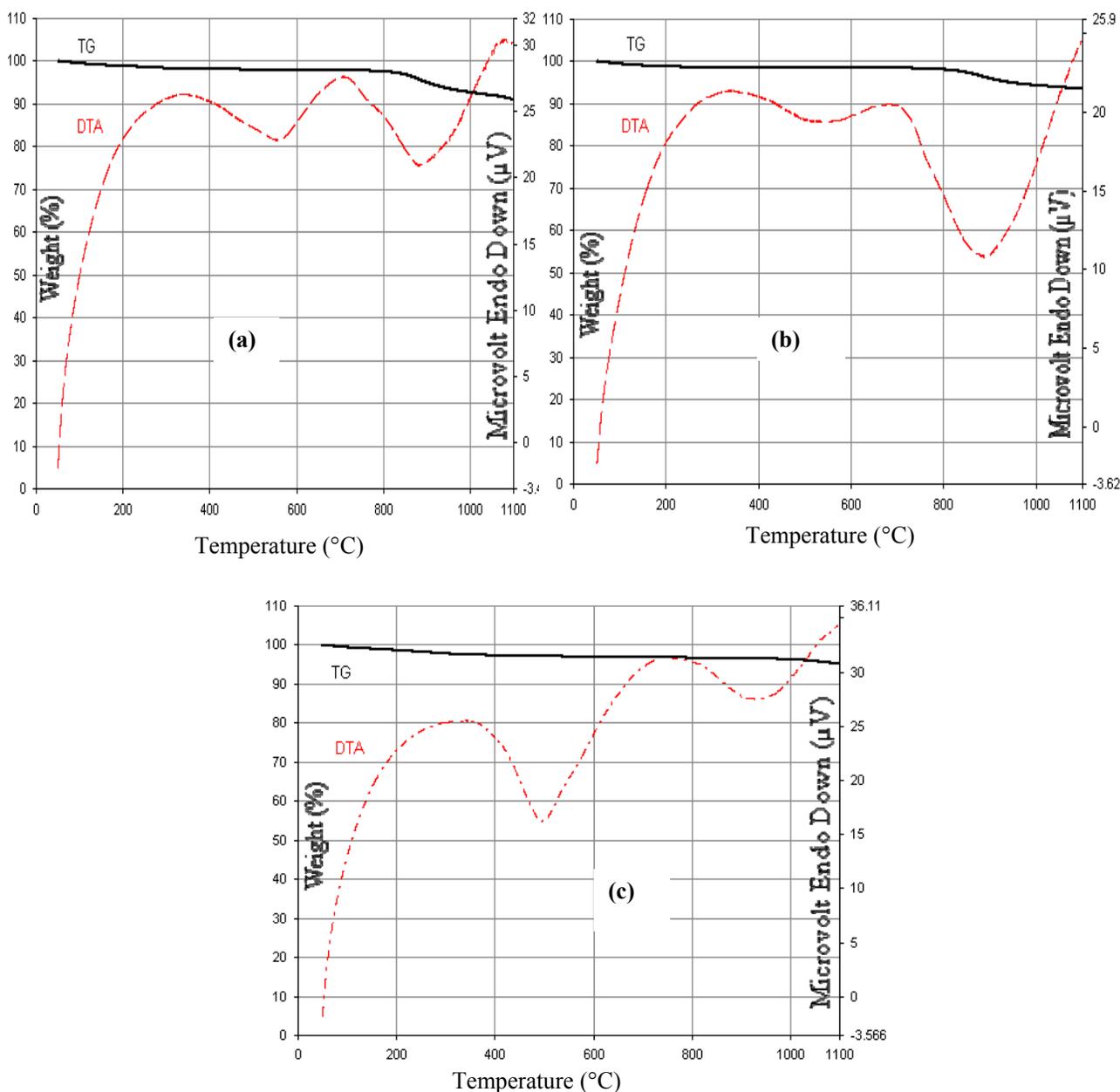
Fig. (7). TGA-DTA patterns for (**a**) meso-TZ-2(500) (**b**) 2% Ni 10% Mo/TZ-2(500) (**c**) 2% Co 8% Mo/TZ-2(500).

NiMo catalysts viz 0.013 mmolg^{-1} and 0.014 mmolg^{-1} respectively (Table **2**). We also observed that calcination temperature has a direct effect on acidic properties of catalysts since the acidity of sample TZ-2(400) is 0.034 mmolg^{-1} which falls down to 0.018 mmolg^{-1} for sample TZ-2(600). Moreover from these results we can speculate the absence of Bronsted sites, since it has been reported that Bronsted sites corresponds to desorption temperatures higher than 400°C [39, 40]. The nature of acid sites is very important property of these catalysts. Low acidity of samples ensures effective dehydrosulfurization over the impregnated samples with minimal cracking and other competing reactions.

3.2. Effect of Support Composition on Catalytic Activity

Hydrodesulfurisation of thiophene was carried out on molybdenum supported TiO₂-ZrO₂ catalysts. The reaction products of thiophene hydrodesulfurization are butane, 1-butene, 2-butene and its isomer, and some amount of 1,3-butadiene but, butene was more selectively formed with always >95% selectivity for all the catalysts studied. Fig. (**9**) shows comparison of the rate of reactions obtained on sulfide CoMo/TZ-2(500) and NiMo/TZ-2(500) catalysts for HDS of thiophene. The order of thiophene conversion at 400°C and atmospheric pressure is CoMo/TZ-2(500) > NiMo/TZ-2(500) and this trend is followed for various metal loadings. These results represent the typical promotional
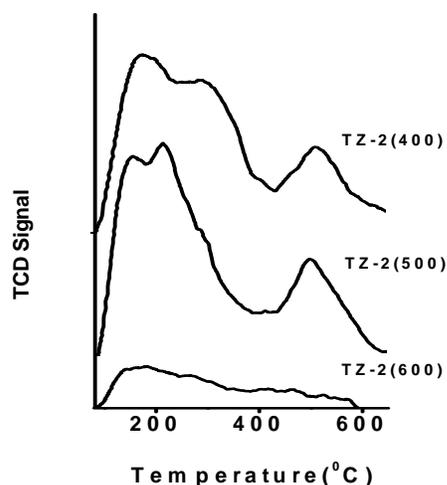
Fig. (8a). TPD analysis of binary titania –zirconia oxides calcined at different temperatures.
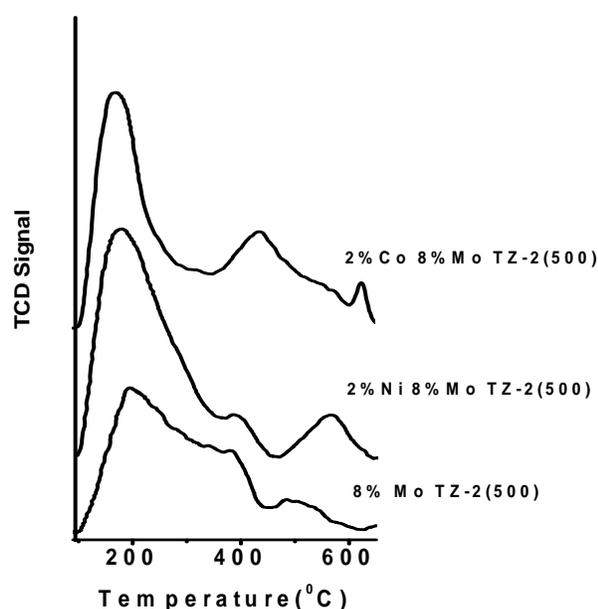
Fig. (8b). TPD analysis of mesoTZ-2(500) with varying composition.

contribution exhibited by Co and Ni, in which the contribution of Co is more than that of Ni. Apart from the TZ-2(500) sample, a comparison with earlier prepared [41] γ-Al$_2$O$_3$ and SBA-15 supported catalysts is shown in Fig. (**9**). The mixed oxide supported catalysts demonstrated superior HDS activity than that shown by SBA-15 and alumina supports; thus the contribution of mixed oxide is evident and

goes well in agreement with the observations reported earlier for the HDS activity using dibenzothiophene as the model compound [17]. Higher activities for modified TiO$_2$ catalysts is not solely due to fine dispersion of the MoS$_2$ phase, the electronic effects due to semiconducting nature of TiO$_2$ may also contribute to enhanced activity. J. Ramirez *et al.* have demonstrated that electronic interaction between the support and the active components can alter the activity and selectivity of the catalysts [42]. We observed that Co loaded catalysts showed better HDS activity than Ni loaded catalysts and highest activity is shown by 2%Co on 8wt%Mo for CoMo catalysts and 2% Ni on 10% Mo for NiMo catalyst.
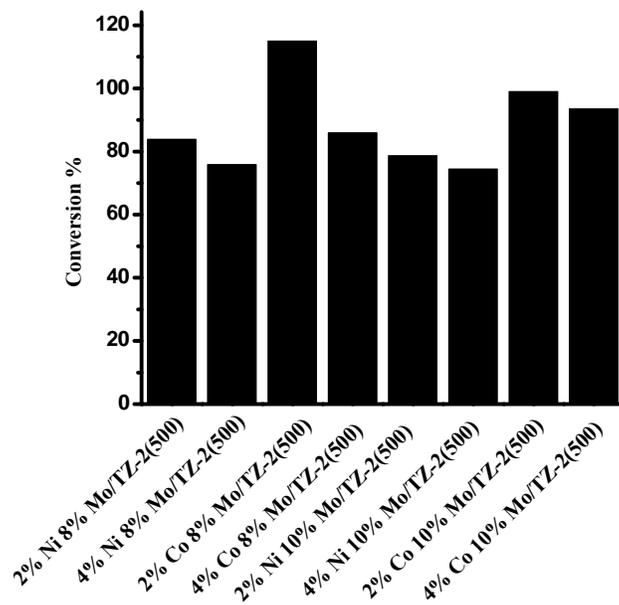
Fig. (9a). Percentage conversion of NiMo,CoMo catalysts on meso-TZ-2(500) with different metallic loadings.

4. CONCLUSION

On the basis of our results of characterization of supports and catalysts as well as activity tests of the catalysts, binary Ti-Zr mixed oxides can be looked upon as an alternative to alumina based supports for hydrodesulfurization. TiO$_2$-ZrO$_2$ binary oxides show better HDS activity than most of the reported catalysts. Favorable metal-support interactions and electronic effects along with moderate acidity would contribute to enhanced activity of titania-zirconia system. This study on the catalytic activity of CoMo and NiMo on

Table 2.   Acidity of Titania-Zirconia and Impregnated Samples

Sample	Total Acidity (mmol/g)	Weak Acidity (mmol/g)	Medium Acidity (mmol/g)	Strong Acidity (mmol/g)
TZ-2(400)	0.034	0.016	0.015	0.003
TZ-2(500)	0.0289	0.0209	0.024	0.004
TZ-2(600)	0.002	-	-	-
2%Co, 8%MoTZ-2(500)	0.013	0.009	0.0003	0.0001
2%Ni, 8%MoTZ-2(500)	0.014	0.012	0.0003	0.002
8% MoTZ-2(500)	0.0275	0.014	0.012	0.0015

TiO_2-ZrO_2 binary supports is expected to lead to the preparation of more active hydrotreatment catalysts.
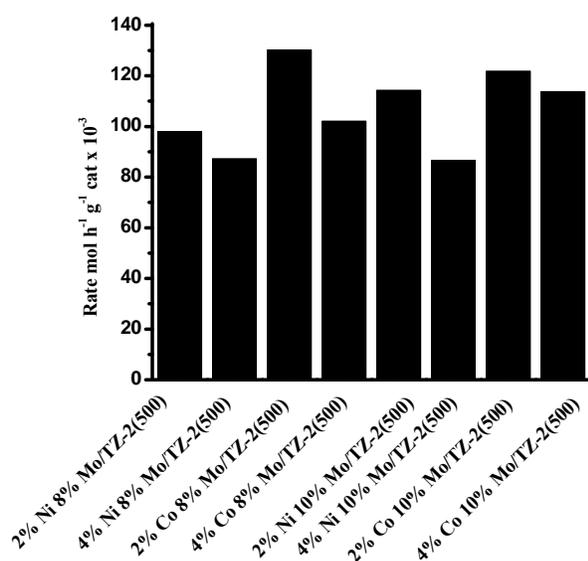
Fig. (9b). Comparison of rate of reactions of meso-TZ-2(500) with different percentages of metallic loadings.
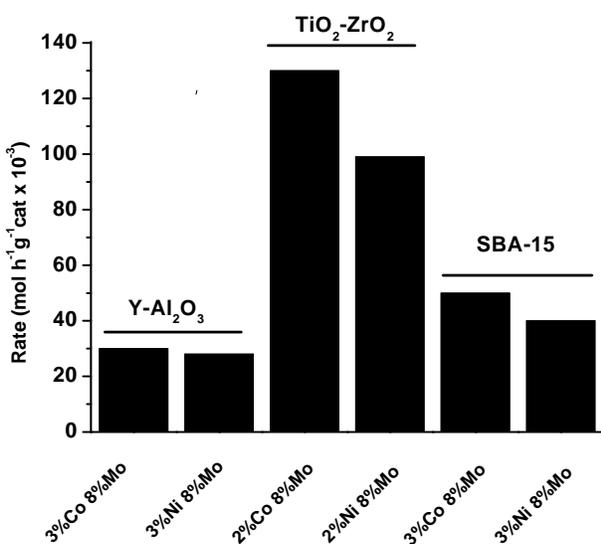
Fig. (9c). Comparison of the catalytic activities of NiMo and CoMo catalysts on meso-TZ-2500, SBA-15 and γ-Al₂O₃.

ACKNOWLEDGEMENTS

CONFLICT OF INTEREST

The authors confirm that this article content has no conflicts of interest.

REFERENCES

[1]   (a) Song, C. An overview of new approaches to deep desulfurization for ultra-clean gasoline, diesel fuel and jet fuel. *Catal. Today.,* **2003**, *86*, 211. (b) Topsoe, H.; Clausen, B.S.; Massoth, F.E. In: *Hydro-treating Catalysis- Science and Technology.* Anderson, J.R.; Baudart, M.; Eds.; Springer- Verlog: New York, Vol.*11,* **1996**.

[2]   Okamoto, Y.; Breysse, M.; Dhar, G.M.; Song, C. Effect of support in hydrotreating catalysis for ultra clean fuel. *Catal. Today,* **2003**, *86*, 1.

[3]   Muralidhar, G.; Srinivas, B.N.; Rana, M.S.; Kumar, M.; Maity, S.K. Mixed oxide supported hydrodesulfurization catalysts - a review. *Catal. Today,* **2003**, *86*, 45.

[4]   Breysse, M.; Afanasiev, P.; Geantet, C.; Vrinat, M. Overview of support effects in hydrotreating catalyst. *Catal. Today,* **2003**, *86*, 5.

[5]   Caero, L.C.; Romero, A.R.; Ramirez, J. Niobium sulfide as a dopant for Mo/TiO₂ catalysts. *Catal. Today,* **2003**, *78* (1-4), 513.

[6]   Barrera, M.C.; Viniegra, M; Escobar, J.; Vrinat, M.; de los Reyes, J.A.; Murrieta, F.; García, J. Highly active MoS₂ on wide-pore ZrO₂–TiO₂ mixed oxides. *Catal. Today,* **2004**, *98* (1-2), 131-139.

[7]   Damyanova, S.; Petrov, L.; Centeno M.A.; Grange, P. Characterization of molybdenum hydrodesulfurization catalysts supported on ZrO₂-Al₂O₃ and ZrO₂-SiO₂ carriers. *Appl. Catal. A. Gen.,* **2002**, *224* (1-2), 271.

[8]   Rana, M.S.; Capitaine, E. M. R.; Leyva, C.; Ancheyta, J. Effect of catalyst preparation and support composition on hydrodesulfurization of dibenzothiophene and Maya crude oil. *Fuel,* **2007**, *86* (9), 1254.

[9]   Rana, M. S.; Maity, S. K.; Ancheyta, J.; Murali Dhar, G.; Prasada Rao, T. S. R. MoCo(Ni)/ZrO₂–SiO₂ hydrotreating catalysts: physico-chemical characterization and activities studies. *Appl. Catal. A. Gen.,* **2004**, *268* (1-2), 89.

[10]   Murali Dhar, G.; Massoth, F.E.; Shabtai, J. Catalytic functionalities of supported sulfides: I. Effect of support and additives on the CoMo catalyst. *J. Catal.,* **1994**, *85*, 52.

[11]   Prins, R. ; de Beer, V.J.H.; Somerjai, G.A. Structure and function of the catalyst and the promoter in Co-Mo hydrodesulfurization catalysts. *Catal. Rev. Sci. Eng.,* **1989**, *31*, 1.

[12]   Maity, S.K.; Srinivas, B.N.; Prasad, V.V.D.N.; Singh, A.; Murali Dhar, G.; Prasada Rao, T.S.R. In: *Recent Advances in Basic and Applied Aspects of Industrial Catalysis.* Prasada Rao, T.S.R.; Murali Dhar, G., Eds.; *Stud. Surf. Sci. Catal.;* Elsevier: Amsterdam. **1998**, vol.*113*, p. 579.

[13]   Wang, A.; Wang, Y.; Kabe, T.; Chen, Y.; Ishihara, A.; Qian, W.; Yao, P. Hydrodesulfurization of dibenzothiophene over siliceous MCM-41-supported catalysts: II. sulfided Ni–Mo catalysts. *J. Catal.,* **2002**, *210*, 319.

[14]   Klimova, T.; Calderon, M.; Ramirez, J. Ni and Mo interaction with Al-containing MCM-41 support and its effect on the catalytic behavior in DBT hydrodesulfurization. *Appl. Catal. A. Gen.,* **2003**, *240*, 29.

[15]   Wang, A.; Wang, Y.; Kabe, T.; Chen, Y.; Ishihara, A.; Qian, W. Hydrodesulfurization of dibenzothiophene over siliceous MCM-41-supported catalysts: I. sulfided Co–Mo catalysts. *J. Catal.,* **2001**, *199*, 19.

[16]   Chiranjeevi, T.; Kumar, P.; Rana, M.S.; Murali Dhar, G.; Prasada Rao, T.S.R. Physico-chemical characterization and catalysis on mesoporous Al-HMS supported molybdenum hydrotreating catalysts. *J. Mol. Catal. A. Chem.,* **2002**, *181*, 109.

[17]   Murali Dhar, G.; Muthu Kumaran, G.; Kumar, M.; Rawat, K.S.; Sharma, L.D.; David Raju, B.; Rama Rao, K.S. Physico-chemical characterization and catalysis on SBA-15 supported molybdenum hydrotreating catalysts. *Catal. Today,* **2005**, *99*, 309-314.

[18]   Li, D.; Nishijima, A.; Morris, D.E. Zeolite-supported Ni and Mo catalysts for hydrotreatments: I. catalytic activity and spectroscopy. *J. Catal.,* **1999**, *182* (2), 339.

[19]   Welters, W.J.J.; Vorbeck, G.; Zandbergen, H.W.; Van de Ven, J.M.; Van Oers, E.M.; de Haan, J.W.; de Beer, V.H.J.; Van Santen, R.A. NaY-supported molybdenum sulfide catalysts: I. catalysts prepared via impregnation with ammonium heptamolybdate. *J. Catal.,* **1996**, *161* (2), 819.

[20]   Muthu, K.G.; Garg, S.; Soni, K.; Kumar, M.; Sharma, L.D.; Murali, D.G.; Rama, R.K.S. Effect of Al-SBA-15 support on catalytic functionalities of hydrotreating catalysts: I. Effect of variation of Si/Al ratio on catalytic functionalities. *Appl. Catal. A. Gen.,* **2006**, *305*, 123-129.

[21]   Muthu, K.G.; Garg, S.; Soni, K.; Kumar, M.; Sharma, L.D.; Rama, R.K.S.; Murali, G. Effect of Al-SBA-15 support on catalytic functionalities of hydrotreating catalysts. II. Effect of variation of molybdenum and promoter contents on catalytic functionalities. *Ind. Eng. Chem. Res.,* **2007**, *46*, 4747-4754.

[22]   Chiranjeevi, T.; Kumar, P.; Maity, S.K.; Rana, M.S.; Murali, D.G.; Prasada Rao, T.S.R. Characterization and hydrodesulfurization

catalysis on WS2 supported on mesoporous Al–HMS material. *Microporous Mesoporous Mater.,* **2001**, *44-45*, 547.

[23] Vradman, L.; Landau, M.V.; Herskowitz, M.; Ezersky, V.; Talianka, M.; Nikitenko, S.; Koltypin, Y.; Gedanken, A. High loading of short WS_2 slabs inside SBA-15: promotion with nickel and performance in hydrodesulfurization and hydrogenation. *J. Catal.,* **2003**, *213*, 163.

[24] Reddy, K.M.; Wei, B.; Song, C. Mesoporous molecular sieve MCM-41 supported Co–Mo catalyst for hydrodesulfurization of petroleum resids. *Catal. Today,* **1998**, *43*, 261-272.

[25] Corma, A.; Martinez, A.; Soria, V.M.; Monton, J.B. Hydrocracking of vacuum gas oil on the novel mesoporous MCM-41 aluminosilicate catalyst. *J. Catal.,* **1995**, *153*, 25-31.

[26] Sampieri, A.; Pronier, S.; Blanchard, J.; Breysse, M.; Brunet, S.; Flyerwerg, F.; Louis, C.; Parot, G. Hydrodesulfurization of dibenzothiophene on MoS_2/MCM-41 and MoS_2/SBA-15 catalysts prepared by thermal spreading of MoO_3. *Catal. Today,* **2005**, *107-108*, 537-544.

[27] Murali Dhar, G.; Srinivas, B.N.; Rana, M.S.; Kumar, M.; Maity, S.K. Mixed oxide supported hydrodesulfurization catalysts-a review. *Catal. Today,* **2003**, *86*, 45-60.

[28] Shimada, H. Morphology and orientation of MoS_2 clusters on Al_2O_3 and TiO_2 supports and their effect on catalytic performance. *Catal. Today,* **2003**, *86*, 17-29.

[29] Ramirez, J.; Fuentes, S.; Diaz, G.; Vrinat, M.; Breysse, M.; Lacroix, M. Hydrodesulphurization activity and characterization of sulphided molybdenum and cobalt – molybdenum catalysts comparision of alumina-, silica-alumina-and titania –supported catalysts. *Appl. Catal. A. Gen.,* **1989**, *52*, 211.

[30] Ramirez, J.; Ruiz-Ramirez, L.; Cedeno, L.; Harle, V.; Vrinat, M.; Breysse, M. Titania-alumina mixed oxides as supports for molybdenum hydrotreating catalysts. *Appl. Catal. A. Gen.,* **1993**, *93*, 163.

[31] Ramirez, J.; Gutierrez-Alejandre, A. Characterization and hydrodesulfurization activity of w-based catalysts supported on Al_2O_3–TiO_2 mixed oxides. *J. Catal.,* **1997**, *170*, 108.

[32] Schacht, P.; Hernandez, G.; Cedeno, L.; Mendoza, J.H.; Ramirez, S.; Garcia, L.; Ancheyta, J. Hydrodesulfurization activity of CoMo catalysts supported on stabilized TiO_2. *Energy Fuels,* **2003**, *17* (1), 1781-1786.

[33] Yuan, Q.; Liu, Y.; Le-Le, L.; Xing, Z.; Chen-Jie, F.; Wen-Tao, D.; Xing-Guo. L; Chun-Hua, Y. Highly ordered mesoporous titania–zirconia photocatalyst for applications in degradation of rhodamine-B and hydrogen evolution. *Microporous Mesoporous Mater.,* **2009**, *124*, 169-178.

[34] Zou, H.; Shen, J.Y. Microcalorimetric and infrared spectroscopic studies of γ-Al2O3 modified by zinc oxide. *Thermochim. Acta,* **2000**, *351*, 165.

[35] Ranjani V. S.; James A. P.; Grover Evans Jr. Spectroscopic characterization of molybdenum-containing zinc titanate desulfurization sorbents. *Ind. Eng. Chem. Res.,* **1994**, *33*, 2810-2818.

[36] Barrera, M.C.; Escobar, J.; de los Reys, J.A.;Cortes, M.A.; Viniegra, M.; Hernandez, A. Effect of solvo-thermal treatment temperature on the properties of sol–gel ZrO_2–TiO_2 mixed oxides as HDS catalyst supports. *Catal. Today,* **2006**, *116*, 498-504.

[37] Li, C.; Li, W.; Zhang, M.; Tao, V. Characterization and catalytic application of homogeneous nano-composite oxides ZrO_2–Al_2O_3. *Catal. Today,* **2004**, *93-95*, 595-601.

[38] Hanafi, S.A.; El-Syed, H.A.; Elmelawy, M.S.; Sultan, E.S.A. Characterization and Catalytic Activities of ZrO_2-TiO_2 Supported Hydrodesulfurization Catalysts. *Pet. Sci. Technol.,* **2009**, *27*, 83-95.

[39] Zou, H.; Lin, Y. S. Structural and surface chemical properties of sol–gel derived TiO_2–ZrO_2 oxides. *Appl. Catal. A.,* **2004**, *265,* 35-42.

[40] Das, D.; Mishra, H.K.; Dalai, A.K.; Parida, K.M. Isopropylation of benzene over sulfated ZrO_2–TiO_2 mixed-oxide catalyst. *Appl. Catal. A Gen.,* **2003**, *243*, 271.

[41] Soni, K.; Rana, B.S.; Sinha, A.K.; Bhaumik, A.; Nandi, M.; Kumar, M.; Dhar, G.M. 3-D ordered mesoporous KIT-6 support for effective hydrodesulfurization catalysts. *Appl. Catal. B. Environ.,* **2009**, *90*, 55-63.

[42] Ramirez, J.; Sanchez-Minero, F. Support effects in the hydrotreatment of model molecules. *Catal. Today,* **2008**, *130*, 267-271.